PHYSICAL REVIEW D **85,** 094010 (2012)

Two-photon form factors of the π^0, η, and η' mesons in the chiral theory with resonances

Henryk Czyż
Institute of Physics, University of Silesia, Katowice PL-40007, Poland

Sergiy Ivashyn and Alexandr Korchin
NSC "Kharkov Institute of Physics and Technology", Kharkov UA-61108, Ukraine

Olga Shekhovtsova
IFIC, Universitat de València-CSIC, Apt. Correus 22085, E-46071 València, Spain
(Received 6 February 2012; published 10 May 2012)

We have developed a phenomenological approach which describes very well the π^0, η and η' meson production in the two-photon interactions. The simultaneous description of the π^0, η and η' meson two-photon form factors is consistent with data in the spacelike region, with the exception of the π^0 *BABAR* data. The obtained form factors are implemented in the event generator EKHARA and the simulated cross sections are presented. Uncertainties in the measured form factors coming from the model dependence in Monte Carlo simulations are studied. The model predictions for the form factor slopes at the origin are given and the high-Q^2 limit is also discussed.

DOI: 10.1103/PhysRevD.85.094010 PACS numbers: 14.40.Be, 13.40.Gp, 13.66.Bc

I. INTRODUCTION

The two-photon transition form factors of the pseudoscalar mesons π^0, η and η' have received a great deal of attention lately—both from the experimental and the theoretical side. The recent *BABAR* experiments [1,2] have provided us with important information in the high-Q^2 region of the photon virtuality and have triggered new insight into the structure of mesons [3–17]. Hopefully, results from Belle experiment will soon be available, and will provide a very important cross-check of the *BABAR* data and boost a progress in the form factor phenomenology. A new experiment KLOE-2 at Frascati [18,19] will soon be able to provide us with the information on the pion two-photon form factor at low Q^2—in a region where no measurements were available [19]. Also, the transition form factors of $\mathcal{P} = \pi^0$, η, η' (and other) mesons will be measured in BES-III [20] experiment at Beijing with high statistics.

The Monte Carlo generators based on reliable models are needed for data analysis and feasibility studies. One of the tools in this field is the Monte Carlo generator EKHARA [21,22], which is already in use by KLOE-2 Collaboration [19]. A reliable simulation has to account for both photon virtualities in the form factor even for a ''single-tag'' experiment. Therefore, the formulas for the form factors as functions of two photon virtualities are needed. This criterion considerably reduces the choice for the form factor, because the majority of the published formulas within different theoretical approaches hold only for the case with one photon being real and the other—spacelike and virtual.

It is worthwhile to stress that the knowledge of the transition form factors is important in itself, but it is also required for the calculation of the hadronic light-by-light scattering part of the anomalous magnetic moment of the muon (a_μ^{LbyL}); see, e.g., [23–26].

In order to take full advantage of the newly planned $g-2$ experiments at Fermilab [27] and J-PARC [28], it is mandatory to improve the accuracy of the hadronic light-by-light contribution. This subject has been recently discussed in detail during the dedicated workshop in Seattle (http://www.int.washington.edu/PROGRAMS/11-47w/). Many important issues related to the $\gamma^*\gamma^*\mathcal{P}$ interaction have recently been discussed in [29].

It has not been feasible so far to develop a rigorous QED/QCD-based theoretical description of the two-photon interaction of mesons, which would be applicable at an arbitrary energy scale. Various methods have been used, depending on the aim of a research: the Brodsky-Lepage (BL) high-Q^2 limit and interpolation formula [30]; the operator product expansion approach to vector-vector-pseudoscalar and vector-vector-axial three-point functions of QCD [31]; the vector meson dominance models [11,32]; the holographic approaches [5,12–14]; the sum rules [7–9,33,34]; the modified perturbative approach [4]; the Regge models [35]; the Dyson-Schwinger equation [36]; the Nambu-Jona-Lasinio model [15,37], the constituent quark models [3,38]; the resonance chiral theory approach [39,40]; and others [16,17]. The research in this field is mainly dedicated to the high-Q^2 region of the form factor with one real and one virtual photon. When one needs to cover a wide range of the photon virtuality, both high-energy and low-energy methods have to be merged in some appropriate way.

The purpose of this paper is twofold: to develop a reliable model able to describe the two-photon form factors of π^0, η and η' mesons with a very small number of

parameters and, then, to implement these form factors in the generator EKHARA.

Our approach is described in Sec. II. We start from the formalism of chiral effective theory with resonances [41–43] as a phenomenological model. The masses of the particles are taken from PDG [44], and the η-η' mixing is accounted for according to Ref. [45,46]. We require that the form factors vanish at high $|t|$. The formulas for the form factors are given in Sec. II A. In Secs. II B and II C we compare the calculated form factors with the experimental results of CELLO [47], CLEO [48] and *BABAR* [1,2] experiments. Furthermore, in Sec. II D, we discuss the implementation of the calculated form factors in the Monte Carlo generator EKHARA [21,22] and simulate the single-tag visible cross section, under conditions similar to those of the CLEO and *BABAR* experiments. The derived formulas allow us to study the high-Q^2 behavior of the form factor (Sec. III A) and the slope of the form factor at the origin (Sec. III B). Finally, in Sec. IV the main conclusions of the paper are drawn.

II. OUR APPROACH AND THE RESULTS

A. Formulas for $F_{\gamma^*\gamma^*\mathcal{P}}$

The two-photon form factor $F_{\gamma^*\gamma^*\mathcal{P}}(t_1, t_2)$ for the meson of type $\mathcal{P} = \pi^0, \eta, \eta'$, encodes the dependence of the amplitude $\mathcal{M}(\gamma^*\gamma^* \to \mathcal{P})$ on the virtuality of the photons ($q_1^2 = t_1$, $q_2^2 = t_2$):

$$\mathcal{M}[\gamma^*(q_1,\nu)\gamma^*(q_2,\beta)\to\mathcal{P}] = e^2\epsilon_{\mu\nu\alpha\beta}q_1^\mu q_2^\alpha F_{\gamma^*\gamma^*\mathcal{P}}(t_1,t_2), \quad (1)$$

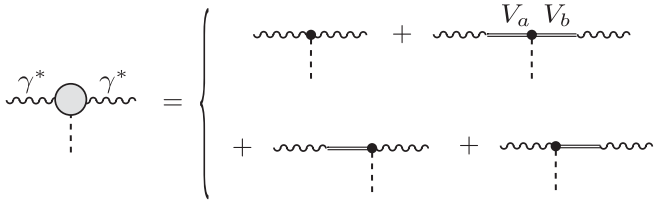

FIG. 1. Diagrams for the $\gamma^*\gamma^*\mathcal{P}$ transition. Dashed lines correspond to the pseudoscalar meson $\mathcal{P}$, solid lines—to the vector mesons and wavy lines to (virtual) photons. $V_a \neq V_b$ for π^0 and $V_a = V_b$ for η and η' form factors.

where $\epsilon_{\mu\nu\alpha\beta}$ is the totally antisymmetric Levi-Civita tensor. Note that $F_{\gamma^*\gamma^*\mathcal{P}}(t_1, t_2) = F_{\gamma^*\gamma^*\mathcal{P}}(t_2, t_1)$ due to Bose symmetry of the photons. We obtain the formulas for the form factors $F_{\gamma^*\gamma^*\mathcal{P}}(t_1, t_2)$ on the basis of the effective chiral Lagrangian [41–43] extended to multioctet resonance contributions, with the η-η' mixing accounted for as in [45,46]. A brief summary of the model is given in Appendix A. We would like to remark that a similar approach was applied in the context of other processes in [49–51].

For simplicity, we neglect the mixing between the octets, which can be added if required by the data. The diagrams describing $\gamma^*\gamma^*P$ transition are presented in Fig. 1. The form factors read

$$F_{\gamma^*\gamma^*\pi^0}(t_1,t_2) = -\frac{N_c}{12\pi^2 f_\pi} + \sum_{i=1}^{n}\frac{4\sqrt{2}h_{V_i}f_{V_i}}{3f_\pi}t_1(D_{\rho_i}(t_1)+D_{\omega_i}(t_1)) + \sum_{i=1}^{n}\frac{4\sqrt{2}h_{V_i}f_{V_i}}{3f_\pi}t_2(D_{\rho_i}(t_2)+D_{\omega_i}(t_2)) - \sum_{i=1}^{n}\frac{4\sigma_{V_i}f_{V_i}^2}{3f_\pi}t_2t_1(D_{\rho_i}(t_2)D_{\omega_i}(t_1)+D_{\rho_i}(t_1)D_{\omega_i}(t_2)), \quad (2)$$

$$F_{\gamma^*\gamma^*\eta}(t_1,t_2) = -\frac{N_c}{12\pi^2 f_\pi}\left(\frac{5}{3}C_q - \frac{\sqrt{2}}{3}C_s\right) + \sum_{i=1}^{n}\frac{4\sqrt{2}h_{V_i}f_{V_i}}{3f_\pi}t_1\left(3C_qD_{\rho_i}(t_1) + \frac{1}{3}C_qD_{\omega_i}(t_1) - \frac{2\sqrt{2}}{3}C_sD_{\phi_i}(t_1)\right) + \sum_{i=1}^{n}\frac{4\sqrt{2}h_{V_i}f_{V_i}}{3f_\pi}t_2\left(3C_qD_{\rho_i}(t_2) + \frac{1}{3}C_qD_{\omega_i}(t_2) - \frac{2\sqrt{2}}{3}C_sD_{\phi_i}(t_2)\right) - \sum_{i=1}^{n}\frac{8\sigma_{V_i}f_{V_i}^2}{f_\pi}t_2t_1\left(\frac{1}{2}C_qD_{\rho_i}(t_2)D_{\rho_i}(t_1) + \frac{1}{18}C_qD_{\omega_i}(t_2)D_{\omega_i}(t_1) - \frac{\sqrt{2}}{9}C_sD_{\phi_i}(t_2)D_{\phi_i}(t_1)\right), \quad (3)$$

$$F_{\gamma^*\gamma^*\eta'}(t_1,t_2) = F_{\gamma^*\gamma^*\eta}(t_1,t_2)\Big|\begin{array}{ll} C_q \to & C_q' \\ C_s \to & -C_s' \end{array}, \quad (4)$$

where n is a number of the vector meson resonance octets. The definitions of all couplings can be found in the Appendix A. The vector meson propagators D_V are

$$D_V(Q^2) = [Q^2 - M_V^2 + i\sqrt{Q^2}\Gamma_{\mathrm{tot},V}(Q^2)]^{-1}. \quad (5)$$

In this paper, we consider only the data in the spacelike region of photon virtuality, thus the modeling of the vector-resonance-energy-dependent widths $\Gamma_{\mathrm{tot},V}(Q^2)$ is not relevant as the widths are equal to zero. We take the values of the masses of all particles according to PDG [44].

We require that the form factors $F_{\gamma^*\gamma^*\mathcal{P}}(t_1, t_2)$ given in (2)–(4) vanish when the photon virtuality t_1 goes to infinity for any value of t_2

$$\lim_{t_1\to-\infty} F_{\gamma^*\gamma^*\mathcal{P}}(t_1, t_2)|_{t_2=\mathrm{const}} = 0. \quad (6)$$

Notice that in this case the conditions

$$\lim_{t\to-\infty} F_{\gamma^*\gamma^*\mathcal{P}}(t, t) = 0, \quad (7)$$

$$\lim_{t\to-\infty} F_{\gamma^*\gamma^*\mathcal{P}}(t, 0) = 0 \quad (8)$$

are automatically satisfied, which is considered a correct short-distance behavior of the form factors (see, for example, discussion in [31]). The constraint (6) leads to the following relations for the couplings:

$$\sqrt{2}h_{V_i}f_{V_i} - \sigma_{V_i}f_{V_i}^2 = 0, \qquad i = 1, \ldots, n, \quad (9)$$

$$-\frac{N_c}{4\pi^2} + 8\sqrt{2}\sum_{i=1}^{n} h_{V_i}f_{V_i} = 0. \quad (10)$$

Therefore, for an ansatz with n vector resonance octets, the two-photon form factors $F_{\gamma^*\gamma^*\mathcal{P}}(t_1, t_2)$ are determined by $2n$ parameters (i.e., the products of the couplings: $f_{V_i}h_{V_i}$ and $\sigma_{V_i}f_{V_i}^2$, $i = 1, \ldots, n$), from which $n - 1$ are to be determined by experiment and the rest $n + 1$ are fixed by (9) and (10). For the one-octet ansatz, there are no free parameters and, in the case of the two-octet ansatz, there is one free parameter.

One of the main objectives of this paper was to develop a reliable model for the $\gamma^*\gamma^*\mathcal{P}$ ($\mathcal{P} = \pi^0$, η, η') transition form factors in the spacelike region, reflecting the experimental data and theoretical constrains and at the same time being as simple as possible. Even if we know that the $SU(3)$ flavor symmetry is broken, we start our investigations using an $SU(3)$-symmetric model (apart from the masses of the mesons, which are fixed at their PDG [44] values) and try to see how many resonance octets we have to include in order to describe the data well. The existing data for the transition form factors in spacelike region [1,2,47,48] come from single tag experiments, where one of the invariants is very close to zero (the one associated with the "untagged" lepton), thus we have information only about $F_{\gamma^*\gamma^*\mathcal{P}}(t, 0)$. It is common to define the $\gamma^*\gamma\mathcal{P}$ form factor $F_{\mathcal{P}}(Q^2, 0) \equiv F_{\gamma^*\gamma^*\mathcal{P}}(t, 0)$ with $Q^2 \equiv -t$ (associated with the "tagged" lepton). From Eqs. (2)–(4) we see that $F_{\mathcal{P}}(Q^2, 0)$ is driven by n parameters (i.e., the products of the couplings: $f_{V_i}h_{V_i}$, $i = 1, \ldots, n$) and there is always only one constraint (10) for any n. Therefore, the number of parameters in $F_{\mathcal{P}}(Q^2, 0)$ to be determined by experiment ("free parameters") equals $n - 1$ (similarly to the case of the $F_{\gamma^*\gamma^*\mathcal{P}}(t_1, t_2)$). In case of the one-octet ansatz there are no free parameters and in the two-octet case there is one free parameter.

B. The one-octet ansatz for the form factors

Let us consider first the one-octet ansatz. In this case,

$$f_{V_1}h_{V_1} = \frac{3}{32\pi^2\sqrt{2}}, \quad (11)$$

and the model gives a prediction for the form factors $F_{\mathcal{P}}(Q^2, 0)$ without any possibility for adjustment. The predictions of this model are compared with experimental data in Figs. 2–4 (dotted line). To quantify the quality of the agreement of the model predictions, we have calculated the χ^2 values for each data set. For the pion transition form factor, the model agrees with CELLO [47] and CLEO [48] and disagrees with the *BABAR* data [1], as can be seen from Table I, which shows the χ^2 values per experiment. For the η and η' transition form factor, the model is in a perfect agreement with CELLO; however for CLEO and *BABAR*, the χ^2 is not good. In total, for the one-octet ansatz we obtain $\chi^2 \approx 358$ for 116 experimental points.

Even though the overall agreement of this simple model with the data is not bad, there is a way to improve it, as will be discussed below.

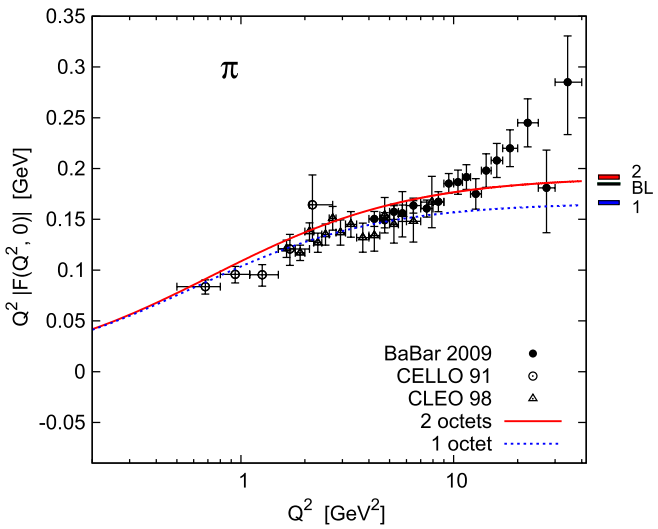

FIG. 2 (color online). Transition form factor $\gamma^*\gamma\pi^0$ compared to the data. The Brodsky-Lepage [30] high-Q^2 limit (BL) is shown as a bold solid straight line at $2 \times f_\pi = 2 \times 0.0924$ GeV. The high-Q^2 limit in our 1-octet ansatz and and 2-octet ansatz are marked as (1) and (2), respectively.

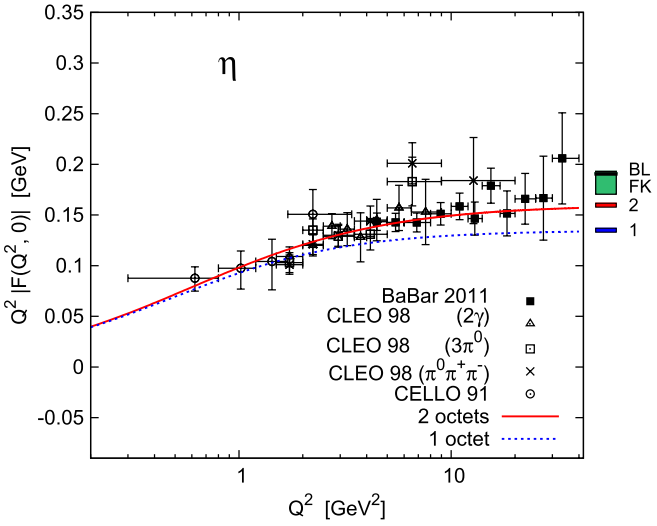

FIG. 3 (color online). Transition form factor $\gamma^*\gamma\eta$ compared to the data. The high-Q^2 limit is shown as a bold solid straight line at $2 \times f_\eta = 2 \times 0.0975$ GeV, according to [3,48] (BL). The limit according to the two-angle η-η' mixing scheme [4,45,46] (FK) is shown as a shaded box (green online) at $0.1705 \ldots 0.1931$ GeV, accounting for the parameter ambiguities (A3). The high-Q^2 limit in our 1-octet ansatz and and 2-octet ansatz are marked as (1) and (2), respectively.

C. The two-octet ansatz for the form factors

In order to make the model more flexible, we include the second vector meson multiplet contributions. We would like to note that there are many known cases when, in order to improve the model predictions, one needs to account for the excited vector resonances, the charged form factor of the pion is among the most famous examples.

In the two-octet ansatz we chose h_{V_1} as a free parameter and determined the value of $f_{V_1} = 0.20173(86)$ using the PDG [44] value for the width

$$\Gamma(\rho \to ee) = \frac{e^4 M_\rho f_{V_1}^2}{12\pi}. \tag{12}$$

The fit to the data gives $\chi^2 \approx 140$ for 116 experimental points. The obtained value of h_{V_1} is

$$h_{V_1} = 0.03121(14), \tag{13}$$

where the error is the parabolic error given by the MINOS package from the MINUIT CERNLIB program. The remaining coupling is given by

$$h_{V_2} f_{V_2} = \frac{3}{32\pi^2\sqrt{2}} - h_{V_1} f_{V_1} = 0.42(5) \times 10^{-3}. \tag{14}$$

The comparison of the two-octet ansatz with the data is also shown in Figs. 2–4 (solid line) and the χ^2 values per experiment are given in Table I. The only data sample which is not in consistency with the model is the *BABAR* data for π^0 [1] (however, for the η and η' transition form factors there is a perfect agreement with *BABAR* data [2]). From the plots in Figs. 2–4 and given the numbers in Table I we conclude that the two-octet calculation is consistent with the bulk of available data.

In principle, the parameter h_{V_1} can be estimated by experiment via the value of the width

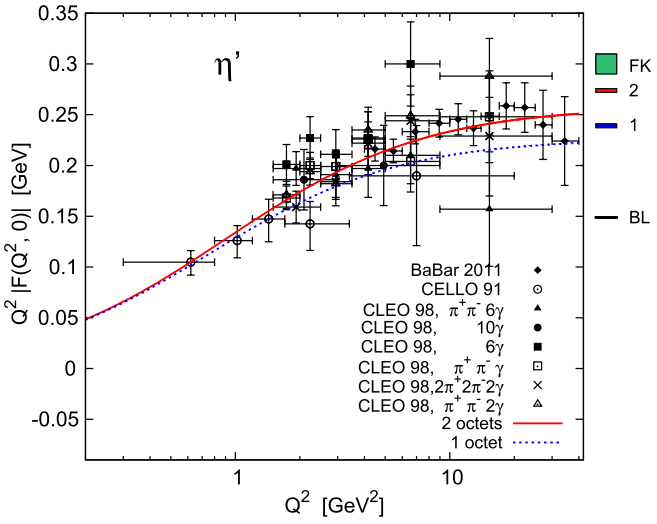

FIG. 4 (color online). Transition form factor $\gamma^*\gamma\eta'$ compared to the data. The high-Q^2 limit is shown as a bold solid straight line at $2 \times f_{\eta'} = 2 \times 0.0744$ GeV, according to [3,48] (BL). The limit according to the two-angle η-η' mixing scheme [4,45,46] (FK) is shown as a shaded box (green online) at $0.29 \ldots 0.31$ GeV, accounting for the parameter ambiguities (A3). The high-Q^2 limit in our 1-octet ansatz and 2-octet ansatz are marked as (1) and (2), respectively.

TABLE I. The χ^2 per experiment and the total χ^2. Number of data points (n.d.p.) is also given for each experiment. In all given experiments the pseudoscalar meson is produced in a two-photon process $e^+e^- \to e^+e^-\mathcal{P}$, but the decay channels for $\mathcal{P}$ identification vary. The "2 octets" column is calculated with the parameter values given by the global fit.

Experiment	1 octet χ^2/n.d.p.	2 octets χ^2/n.d.p.
CELLO ($\pi^0 \to \gamma\gamma$)	0.29/5	0.47/5
CLEO ($\pi^0 \to \gamma\gamma$)	6.27/15	20.96/15
BABAR ($\pi^0 \to \gamma\gamma$)	124.83/17	55.85/17
CELLO ($\eta \to \gamma\gamma$)	0.24/4	0.13/4
CLEO ($\eta \to \pi^+\pi^-\pi^0$)	19.28/6	11.13/6
CLEO ($\eta \to \gamma\gamma$)	8.55/8	2.10/8
CLEO ($\eta \to \pi^0\pi^0\pi^0$)	10.91/5	5.63/5
BABAR ($\eta \to \gamma\gamma$)	89.02/11	9.34/11
CELLO ($\eta' \to \gamma\gamma$)	0.11/5	0.29/5
CLEO ($\eta' \to \gamma\gamma\pi^+\pi^-$)	19.90/6	7.48/6
CLEO ($\eta' \to \gamma\gamma\pi^+\pi^-\pi^+\pi^-$)	2.61/5	1.44/5
CLEO ($\eta' \to \gamma\pi^+\pi^-$)	14.01/6	4.64/6
CLEO ($\eta' \to 6\gamma$)	21.54/5	12.62/5
CLEO ($\eta' \to 10\gamma$)	0.49/2	0.23/2
CLEO ($\eta' \to \pi^+\pi^-6\gamma$)	5.93/5	4.80/5
BABAR ($\eta' \to \gamma\gamma$)	33.87/11	3.10/11
total	357.87/116	140.22/116

TABLE II. The $\rho \to \pi\gamma$ decay width uncertainty and the corresponding values of h_{V_1}.

Decay	Width	Reference	h_{V_1}
$\rho^0 \to \pi^0\gamma$	89(12) keV	PDG [44]	0.041(3)
$\rho^0 \to \pi^0\gamma$	77(20) keV	SND [52]	0.038(5)
$\rho^+ \to \pi^+\gamma$	68(7) keV	PDG [44]	0.036(2)

$$\Gamma(\rho^0 \to \pi^0\gamma) = \frac{4\alpha M_\rho^3 h_{V_1}^2}{27 f_\pi^2}\left(1 - \frac{m_\pi^2}{M_\rho^2}\right)^3. \quad (15)$$

Using the PDG [44] values for the width (15), one obtains

$$h_{V_1} = 0.041(3), \quad (16)$$

which is in tension with the value given by fit (13). This might be a result of neglecting the higher octets or omission of the $SU(3)$ flavor-breaking effects. In order to check this, we have added the third octet to the model and fitted two free parameters: h_{V_1} and $h_{V_2} f_{V_2}$. The fit to the experimental data gives $\chi^2 \approx 136$ for 116 experimental points, so there is no essential improvement in the description of data by the model. The fit gives $h_{V_1} = 0.03279(75)$ and $h_{V_2} f_{V_2} = -0.73(54) \times 10^{-3}$. Finally, for the couplings of the third octet, one gets $h_{V_3} f_{V_3} = \frac{3}{32\pi^2\sqrt{2}} - h_{V_1} f_{V_1} - h_{V_2} f_{V_2} \approx 7.45 \times 10^{-3}$. In this fit, we observe a very high correlation between the parameters h_{V_1} and $h_{V_2} f_{V_2}$ with the off-diagonal correlation coefficient equal to -0.99. Notice that h_{V_1} is almost unchanged as compared to (13) and we conclude that in order to accommodate the value (16) in this model we would need to allow for couplings which break the $SU(3)$ flavor symmetry. This is, however, beyond the scope of the present paper. We leave the possible refinements of the model for further investigations.

In context of the discrepancy between (13) and (16), we would like to illustrate the actual experimental uncertainty in the ρ meson decay width. In Table II we show the values of h_{V_1}, which are deduced from different experimental values of the width: the PDG constrained fit [44] for $\Gamma(\rho^0 \to \pi^0\gamma)$; the SND measurement [52] for $\Gamma(\rho^0 \to \pi^0\gamma)$; the PDG constrained fit and average [44] for $\Gamma(\rho^+ \to \pi^-\gamma)$.

D. The Monte Carlo simulation

We have implemented the transition form factors obtained within the two-octet model described above into the Monte Carlo generator EKHARA (http://prac.us.edu.pl/\%7Eekhara). From the technical point of view of the event generation, it is a straightforward generalization because the mappings used in [21] for π^0 work similarly well also for η and η'.

We simulate the cross sections $d\sigma/dQ^2$ for the process $e^+e^- \to e^+e^-\mathcal{P}$ and compare the results with existing "single-tag" data from the CELLO [47], CLEO [48] and *BABAR* [1,2] experiments. In a single-tag experiment, the tagged lepton fixes the value of $Q^2 = -t_1$ and the 4-momentum squared of the untagged lepton $t_2 = -q_2^2$ is kinematically restricted to near zero. For example, in the *BABAR* experiment, the actual thresholds for q_2^2 are 0.18 GeV^2 for pions [1] and 0.38 GeV^2 for η and η' [2], due to the imposed event selection. The experimental $d\sigma/dQ^2$ is given within these cuts, and, therefore, the simulated $d\sigma/dQ^2$ is computed within the similar event selection. As expected, a good agreement between the generator predictions and the data [2,48] is observed; see Figs. 5 and 6. The tension between the π^0 *BABAR* data [1] and the results of simulations is similar to the one observed for the form factor in Fig. 2.

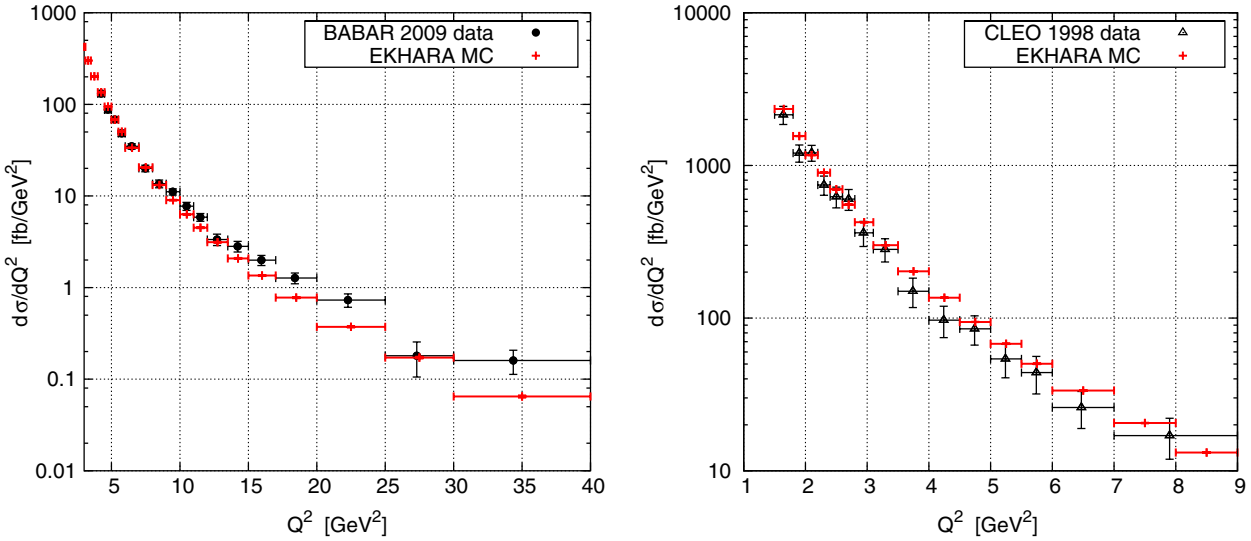

FIG. 5 (color online). The cross section $d\sigma/dQ^2$ for the process $e^+e^- \to e^+e^-\pi^0$ compared to *BABAR* [1] (left) and CLEO [48] (right).

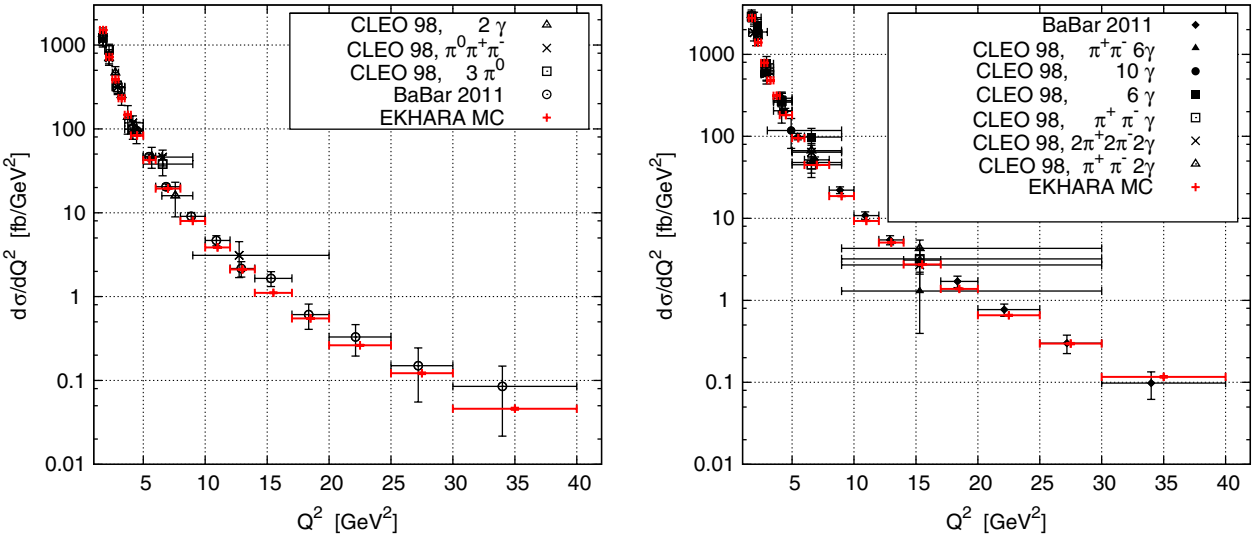

FIG. 6 (color online). The cross section $d\sigma/dQ^2$ for the process $e^+e^- \to e^+e^-\eta$ (left) and $e^+e^- \to e^+e^-\eta'$ (right) compared to CLEO [48] and *BABAR* [2] data.

An important note is in order here. The values of the $d\sigma/dQ^2$ are the primary results of the experiment. The form factor $F_{\mathcal{P}}(Q^2, 0)$ is calculated then on the basis of the measured $d\sigma/dQ^2$ and the simulation. It is known that the model dependence in the simulation leads to the uncertainty in the form factor, which is "measured" in this way. In the *BABAR* analyses, the corresponding uncertainties in cross section are estimated to be at the level of 3.5% for pions [1] and 4.6% for η and η' [2] (based on the simulation with the q_2^2-dependent and q_2^2-independent form factors). As stressed in [1], this uncertainty is very sensitive to the actual q_2^2 cut.

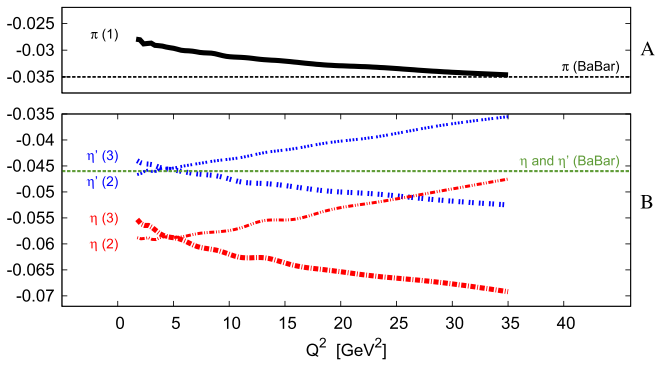

FIG. 7 (color online). The relative difference of the cross sections $(d\sigma[\text{full}] - d\sigma[\text{approx}])/d\sigma[\text{full}]$ for the process $e^+e^- \to e^+e^-\pi^0$ (A) and $e^+e^- \to e^+e^-\eta^{(\prime)}$ (B). The approximate simulation ($d\sigma$[approx]) ignores the form factor dependence on the momentum transfer (q_2^2) to the untagged lepton. The full simulation ($d\sigma$[full]) accounts for the virtuality of both photons in the form factor. The following cuts are used in the simulation: (1) $|q_2^2| < 0.18$ GeV^2 [1]; (2) $|\cos\theta^*_{e\mathcal{P}}| > 0.99$ and $|q_2^2| < 0.6$ GeV^2 [2]; (3) $|q_2^2| < 0.38$ GeV^2 [2]. The lines denoted by (*BABAR*) show estimates for the relative difference, as given in the *BABAR* papers: for π^0—in [1], for η and η'—in [2].

Recently, the effects of the q_2^2 cut were emphasized on the level of the form factor considerations [11]. The Monte Carlo generator in hand allows us to perform a more conclusive study, namely, to investigate the magnitude of the cross section uncertainties, discussed above. Similarly to the method used in the *BABAR* [1,2] analyses we perform two simulations: the first ($d\sigma$[full]$/dQ^2$) with the exact form factor $F_{\gamma^*\gamma^*\mathcal{P}}(t_1, t_2)$ and the second ($d\sigma$[approx]$/dQ^2$) with the approximated form factor $F_{\gamma^*\gamma^*\mathcal{P}}(t_1, t_2) \approx F_{\gamma^*\gamma\mathcal{P}}(t_1, 0)$, i.e., neglecting the momentum transfer to the untagged lepton in the form factor. The relative difference of the corresponding cross sections is then plotted in Fig. 7. Our estimations for the uncertainty are in a rough agreement with that of *BABAR* [1,2]. However, in contrast to the estimate of *BABAR*, a dependence of this uncertainty on Q^2 is observed in our simulation. If this effect is not accounted for in the data it might result in inducing a fake Q^2 dependence of the form factor.

In order to investigate the impact of the event selection on the error estimate, we perform the simulation for η and η' mesons with the direct cut on the second (untagged) invariant (q_2^2) and separately with the cut on the angle between the initial and final untagged lepton ($|\cos\theta^*_{e\mathcal{P}}| > 0.99$), which effectively induces the cut on q_2^2 [1,2]. From Fig. 7 we see that the error estimate and its Q^2 dependence is very sensitive to the event selection.

III. THE LIMITS OF THE FORM FACTORS

A. The high-Q^2 limit of the form factors

The issue of the asymptotic behavior of the form factors usually deserves an attention. In our approach, the high-Q^2 limits ($t \to -\infty$) are the following. In case of the one-octet ansatz, we obtain from Eqs. (2)–(4)

$$F_{\gamma^*\gamma\pi^0}(t,0) = \frac{1}{8\pi^2 f_\pi}\frac{1}{t}(M_\rho^2 + M_\omega^2) + \mathcal{O}\left(\frac{1}{t^2}\right), \quad (17)$$

$$F_{\gamma^*\gamma^*\pi^0}(t,t) = \frac{1}{4\pi^2 f_\pi}\frac{1}{t^2}M_\rho^2 M_\omega^2 + \mathcal{O}\left(\frac{1}{t^3}\right), \quad (18)$$

$$F_{\gamma^*\gamma\eta}(t,0) = \frac{1}{8\pi^2 f_\pi}\frac{1}{t}\left(3C_q M_\rho^2 + \frac{1}{3}C_q M_\omega^2 - \frac{2\sqrt{2}}{3}C_s M_\phi^2\right) + \mathcal{O}\left(\frac{1}{t^2}\right), \quad (19)$$

$$F_{\gamma^*\gamma^*\eta}(t,t) = \frac{1}{8\pi^2 f_\pi}\frac{1}{t^2}\left(3C_q M_\rho^4 + \frac{1}{3}C_q M_\omega^4 - \frac{2\sqrt{2}}{3}C_s M_\phi^4\right) + \mathcal{O}\left(\frac{1}{t^3}\right). \quad (20)$$

In case of the two-octet ansatz, we obtain

$$F_{\gamma^*\gamma\pi^0}(t,0) = \frac{4\sqrt{2}}{3f_\pi}\frac{1}{t}[h_{V_1}f_{V_1}(M_\rho^2 + M_\omega^2) + h_{V_2}f_{V_2}(M_{\rho'}^2 + M_{\omega'}^2)] + \mathcal{O}\left(\frac{1}{t^2}\right), \quad (21)$$

$$F_{\gamma^*\gamma^*\pi^0}(t,t) = \frac{8\sqrt{2}}{3f_\pi}\frac{1}{t^2}[h_{V_1}f_{V_1}M_\rho^2 M_\omega^2 + h_{V_2}f_{V_2}M_{\rho'}^2 M_{\omega'}^2] + \mathcal{O}\left(\frac{1}{t^3}\right), \quad (22)$$

$$F_{\gamma^*\gamma\eta}(t,0) = \frac{4\sqrt{2}}{3f_\pi}\frac{1}{t}\left[h_{V_1}f_{V_1}\left(3C_q M_\rho^2 + \frac{1}{3}C_q M_\omega^2 - \frac{2\sqrt{2}}{3}C_s M_\phi^2\right) + h_{V_2}f_{V_2}\left(3C_q M_{\rho'}^2 + \frac{1}{3}C_q M_{\omega'}^2 - \frac{2\sqrt{2}}{3}C_s M_{\phi'}^2\right)\right] + \mathcal{O}\left(\frac{1}{t^2}\right), \quad (23)$$

$$F_{\gamma^*\gamma^*\eta}(t,t) = \frac{8\sqrt{2}}{3f_\pi}\frac{1}{t^2}\left[h_{V_1}f_{V_1}\left(3C_q M_\rho^4 + \frac{1}{3}C_q M_\omega^4 - \frac{2\sqrt{2}}{3}C_s M_\phi^4\right) + h_{V_2}f_{V_2}\left(3C_q M_{\rho'}^4 + \frac{1}{3}C_q M_{\omega'}^4 - \frac{2\sqrt{2}}{3}C_s M_{\phi'}^4\right)\right] + \mathcal{O}\left(\frac{1}{t^3}\right). \quad (24)$$

The limits for the η' form factor can be obtained from the above formulas according to (4).

The expressions (21) and (23) guide the high-Q^2 behavior of the form factors measured in single-tag experiments (shown in Figs. 2–4). We see that, in our approach, the asymptotic value of $Q^2|F_{\mathcal{P}}(Q^2,0)|$ depends not only on the mixing parameters and decay constants but also on the masses of the vector resonances. Numerically, for π^0 transition form factor, the value of $Q^2|F_{\pi^0}(Q^2,0)|$ in our approach with two octets is very close to that of the Brodsky-Lepage [30] high-Q^2 limit $Q^2|F_{\pi^0}(Q^2,0)| \to 2f_\pi$, shown as a bold solid line (BL) in Fig. 2.

The perturbative QCD prediction for the asymptotic of the η and η' form factors is often given in a simple approach in terms of the parameters $f_\eta = 0.0975$ GeV and $f_{\eta'} = 0.0744$ GeV [3,48]: $Q^2|F_{\eta^{(\prime)}}(Q^2,0)| \to 2f_{\eta^{(\prime)}}$. These values are shown as bold solid line (BL) in Figs. 3 and 4 and in this case one can notice no coincidence with the values given by (23). Sometimes it is also called the Brodsky-Lepage limit, with a reference to [53]. However, we would like to remark that in [53] the $SU(3)$ flavor-breaking effects are not considered and the assumed η-η' mixing may be not consistent with modern data. An attempt to interpret the results of [53] by means of $f_{\eta'} = 0.0744$ GeV is in tension with the data for η' form factor, as one can see in Fig. 4 and as noticed in [3].

In principle, there are other ways to apply the formulas of [53] to the form factors of physical states η and η' [54]. For example, the limit for the η and η' transition form factors can be calculated according to the Feldman-Kroll (FK) two-angle η-η' mixing scheme [4,46]. The latter values are shown as a shaded box (FK) in Figs. 3 and 4 (green online). Notice that numerically this limit for η meson is very close to that of BL approach and also to the value given by our model; however, for η' all the three values are different.

B. The slope of the form factor at the origin

Sometimes it is convenient to define the so-called slope of the transition form factor at the origin $a_{\mathcal{P}}$ (''slope parameter'')

$$a_{\mathcal{P}} \equiv \frac{1}{F_{\gamma^*\gamma^*\mathcal{P}}(0,0)}\frac{dF_{\gamma^*\gamma^*\mathcal{P}}(t,0)}{dx}\bigg|_{t=0}, \quad (25)$$

where $x \equiv t/m_{\mathcal{P}}^2$. Notice that being defined this way, $a_{\mathcal{P}}$ is a dimensionless quantity, which is related to the effective region of the $\gamma\gamma^*\mathcal{P}$ interaction $\langle r_{\mathcal{P}}^2\rangle = 6a_{\mathcal{P}}/m_{\mathcal{P}}^2$. The average experimental value for a_π listed in PDG [44] (linear coefficients of the π^0 electromagnetic form factor) is mainly driven not by a direct measurement, but by an extrapolation done in Ref. [47]. The direct measurements of a_π are less precise [55,56]. The experimental knowledge of a_η is much better and recently the new experiments contributed: MAMI-C [57] and NA60 [58,59]. For $a_{\eta'}$, we were not able to find a result of a direct measurement.

From Eqs. (2)–(4) one obtains the following model prediction for the slope parameters:

$$a_\pi = \frac{16\sqrt{2}\pi^2 m_\pi^2}{N_C}\sum_{i=1}^{n} h_{V_i}f_{V_i}\left(\frac{1}{M_{\rho_i}^2} + \frac{1}{M_{\omega_i}^2}\right), \quad (26)$$

TABLE III. Model prediction for the slope parameters $a_{\mathcal{P}}$ and two most recent experimental values. The "2 octets" column is calculated with the parameter values given by our global fit. The first error in experimental value is due to statistics and the second one is systematics.

	1 octet	2 octets	Experiments	
a_π	0.03003(1)	0.02870(9)	0.026(24) (48) [55]	0.025(14) (26) [56]
a_η	0.546(9)	0.521(2)	0.576(105) (39) [57]	0.585(18) (13) [59]
$a_{\eta'}$	1.384(3)	1.323(4)	...	...

$$a_\eta = \frac{16\sqrt{2}\pi^2 m_\eta^2}{N_C}\left(\frac{5}{3}C_q - \frac{\sqrt{2}}{3}C_s\right)^{-1} \times \sum_{i=1}^{n} h_{V_i} f_{V_i}\left(\frac{3C_q}{M_{\rho_i}^2} + \frac{C_q}{3M_{\omega_i}^2} - \frac{2\sqrt{2}C_s}{3M_{\phi_i}^2}\right), \quad (27)$$

$$a_{\eta'} = \frac{16\sqrt{2}\pi^2 m_{\eta'}^2}{N_C}\left(\frac{5}{3}C'_q + \frac{\sqrt{2}}{3}C'_s\right)^{-1} \times \sum_{i=1}^{n} h_{V_i} f_{V_i}\left(\frac{3C'_q}{M_{\rho_i}^2} + \frac{C'_q}{3M_{\omega_i}^2} + \frac{2\sqrt{2}C'_s}{3M_{\phi_i}^2}\right). \quad (28)$$

The numerical values for $a_{\mathcal{P}}$ are listed in Table III. On its basis, we conclude that there is a reasonable agreement between model predictions and experiments.

We would like to remark that in the limit of the equal masses for vector resonances within the octet, Eqs. (26)–(28) lead to the following relation between the slope parameters: $a_\pi/m_\pi^2 = a_\eta/m_\eta^2 = a_{\eta'}/m_{\eta'}^2$.

IV. SUMMARY

Using the scheme of the η-η' mixing with two decay parameters (f_0 and f_8) and two mixing angles (θ_0, θ_8) [45,46] and following the approach of chiral effective theory with resonances [41–43], we derive the expressions for the two-photon transition form factors of the $\mathcal{P} = \pi^0,\ \eta,\ \eta'$ mesons. The tree-level contributions within this effective field theory approach are considered. For the case of the one-octet ansatz, there are no free parameters and we obtain the model prediction for the form factors. For the case of the two-octet ansatz, the model parameter is fitted to the data. We find that the two-octet calculation is consistent with the bulk of available data but cannot accommodate the π^0 *BABAR* data [1]. The high-Q^2 limits of the form factors in our approach are compared to those of the Brodsky and Lepage [3,30,48] and to those of Feldmann and Kroll [4,46]. The slope of the transition form factor at the origin, $a_{\mathcal{P}}$, is calculated and compared to available data. A reasonable agreement between model predictions and experiments is found.

The obtained form factors are implemented in the EKHARA Monte Carlo generator. As a test of the generator, the cross section $d\sigma/dQ^2$ is simulated for the process $e^+e^- \to e^+e^-\mathcal{P}$ and compared to data using the event selections, which mimic the "single-tag" experimental conditions.

Using the Monte Carlo simulation, we investigate the impact of neglecting the momentum transfer to the untagged lepton (t_2) on the cross section and form factor measurements. The uncertainty in the visible cross section due to the simplification of the form factor $F_{\gamma^*\gamma^*\mathcal{P}}(t_1, t_2) \approx F_{\gamma^*\gamma^*\mathcal{P}}(t_1, 0)$ is estimated for the phase space cuts similar to the experimental ones.

Because of very small number of free parameters and good agreement with data, the approach presented in this work is a good starting point for further model adjustments, e.g., for including the $SU(3)$ flavor symmetry-breaking in the couplings. Using the developed generator one will be able to study, e.g., a possible manifestation of such effects in the cross section $d\sigma/dQ^2$ within a realistic phase space cuts.

ACKNOWLEDGMENTS

We would like to kindly acknowledge our colleagues from experimental collaborations, whose feedback about the EKHARA generator and the physics case of $e^+e^- \to e^+e^-\mathcal{P}$ gave a motivation of the current research. We greatly profited from discussions with Danilo Babusci, Achim Denig, Dario Moricciani, Matteo Mascolo, Elisabeta Prencipe and Graziano Venanzoni. We also thank Fred Jegerlehner and Andreas Nyffeler for discussions. This research was partly supported by Marie Curie Intra European Fellowship within the 7th European Community Framework Program (FP7-PEOPLE-2009-IEF), by Polish Ministry of Science and High Education from budget for science for years 2010–2013, Grant No. N N202 102638, by National Academy of Science of Ukraine under Contract Nos. 50/53-2011 and 50/53-2012, by Sonderforschungsbereich SFB1044 of the Deutsche Forschungsgemeinschaft, by Spanish Consolider Ingenio 2010 Program CPAN (CSD2007-00042) as well by MEC (Spain) under Grant Nos. FPA2007-60323, FPA2011-23778. This work is a part of the activity of the "Working Group on Radiative Corrections and Monte Carlo Generators for Low Energies" (http://www.lnf.infn.it/wg/sighad/) [62].

APPENDIX A: FORMALISM

The lightest pseudoscalar mesons are supposed to play the role of the (pseudo-)Nambu-Goldstone boson fields of spontaneously $G = SU(3)_L \times SU(3)_R$ to $H = SU(3)_V$ broken symmetry. To introduce the physical states η and η' we choose the scheme with two mixing angles (θ_0, θ_8); see [45,46]. The nonet of the pseudoscalar mesons reads

$$u = \exp\left\{\frac{i}{\sqrt{2}f_\pi}\begin{pmatrix} \frac{\pi^0+C_q\eta+C_q'\eta'}{\sqrt{2}} & \pi^+ & \frac{f_\pi}{f_K}K^+ \\ \pi^- & \frac{-\pi^0+C_q\eta+C_q'\eta'}{\sqrt{2}} & \frac{f_\pi}{f_K}K^0 \\ \frac{f_\pi}{f_K}K^- & \frac{f_\pi}{f_K}\bar{K}^0 & -C_s\eta + C_s'\eta' \end{pmatrix}\right\}, \tag{A1}$$

where f_π and f_K are the pion and kaon decay constants and the following notation is used

$$\begin{aligned} C_q &\equiv \frac{f_\pi}{\sqrt{3}\cos(\theta_8-\theta_0)}\left(\frac{1}{f_8}\cos\theta_0 - \frac{1}{f_0}\sqrt{2}\sin\theta_8\right), & C_q' &\equiv \frac{f_\pi}{\sqrt{3}\cos(\theta_8-\theta_0)}\left(\frac{1}{f_0}\sqrt{2}\cos\theta_8 + \frac{1}{f_8}\sin\theta_0\right), \\ C_s &\equiv \frac{f_\pi}{\sqrt{3}\cos(\theta_8-\theta_0)}\left(\frac{1}{f_8}\sqrt{2}\cos\theta_0 + \frac{1}{f_0}\sin\theta_8\right), & C_s' &\equiv \frac{f_\pi}{\sqrt{3}\cos(\theta_8-\theta_0)}\left(\frac{1}{f_0}\cos\theta_8 - \frac{1}{f_8}\sqrt{2}\sin\theta_0\right). \end{aligned} \tag{A2}$$

Fixing the angles θ_0, θ_8 and constants f_0, f_8 [45,46],

$$\theta_8 = -21.2^\circ \pm 1.6^\circ, \qquad \theta_0 = -9.2^\circ \pm 1.7^\circ, \qquad f_8 = (1.26 \pm 0.04)f_\pi, \qquad f_0 = (1.17 \pm 0.03)f_\pi, \tag{A3}$$

and taking $f_\pi = 92.4$ MeV, one obtains $C_q \approx 0.720$, $C_s \approx 0.471$, $C_q' \approx 0.590$ and $C_s' \approx 0.576$. Notice that, according to notation (A1), the couplings of the η' are easily related to those of the η meson by means of substitution

$$C_q \to C_q', \qquad C_s \to -C_s'. \tag{A4}$$

Obviously, this pattern also holds in the expressions for the form factors in our approach.

At the lowest order, the Wess-Zumino-Witten Lagrangian [60,61], which describes the interaction of pseudoscalar mesons with two photons, can be written down in the terms of the physical fields as

$$\mathcal{L}_{\gamma\gamma P} = -\frac{e^2N_c}{24\pi^2 f_\pi}\epsilon^{\mu\nu\alpha\beta}\partial_\mu B_\nu \partial_\alpha B_\beta\left[\pi^0 + \eta\left(\frac{5}{3}C_q - \frac{\sqrt{2}}{3}C_s\right) + \eta'\left(\frac{5}{3}C_q' + \frac{\sqrt{2}}{3}C_s'\right)\right], \tag{A5}$$

where $N_c = 3$ is the number of quark colors and the electromagnetic field is denoted by B_ν.

Assuming the $SU(3)$ symmetry for the coupling constants of the vector mesons, the γV interaction is written as

$$\mathcal{L}_{\gamma V} = -e\sum_{i=1}^{n} f_{V_i}\partial_\mu B_\nu\left(\tilde{\rho}_i^{\mu\nu} + \frac{1}{3}\tilde{\omega}_i^{\mu\nu} - \frac{\sqrt{2}}{3}\tilde{\phi}_i^{\mu\nu}\right), \tag{A6}$$

where we have summed over octets of the vector mesons, $\tilde{V}_{\mu\nu} \equiv \partial_\mu V_\nu - \partial_\nu V_\mu$, f_{V_i} is the (dimensionless) coupling for the vector representation of the spin-1 fields for a fixed octet.

The Lagrangians that describe vector-photon-pseudoscalar and two vector mesons interactions with pseudoscalar [43] in the terms of the physical fields read

$$\begin{aligned} \mathcal{L}_{V\gamma\mathcal{P}} = &-\sum_{i=1}^{n}\frac{4\sqrt{2}eh_{V_i}}{3f_\pi}\epsilon_{\mu\nu\alpha\beta}\partial^\alpha B^\beta[(\rho_i^\mu + 3\omega_i^\mu)\partial^\nu\pi^0 + [(3\rho_i^\mu + \omega_i^\mu)C_q + 2\phi_i^\mu C_s]\partial^\nu\eta \\ &+ [(3\rho_i^\mu + \omega_i^\mu)C_q' - 2\phi_i^\mu C_s']\partial^\nu\eta'], \end{aligned} \tag{A7}$$

$$\begin{aligned} \mathcal{L}_{VV\mathcal{P}} = -\sum_{i=1}^{n}\frac{4\sigma_{V_i}}{f_\pi}\epsilon_{\mu\nu\alpha\beta}\Bigg[&\pi^0\partial^\mu\omega_i^\nu\partial^\alpha\rho_i^\beta + \eta\left[(\partial^\mu\rho_i^\nu\partial^\alpha\rho_i^\beta + \partial^\mu\omega_i^\nu\partial^\alpha\omega_i^\beta)\frac{1}{2}C_q - \partial^\mu\phi_i^\nu\partial^\alpha\phi_i^\beta\frac{1}{\sqrt{2}}C_s\right] \\ &+ \eta'\left[(\partial^\mu\rho_i^\nu\partial^\alpha\rho_i^\beta + \partial^\mu\omega_i^\nu\partial^\alpha\omega_i^\beta)\frac{1}{2}C_q' + \partial^\mu\phi_i^\nu\partial^\alpha\phi_i^\beta\frac{1}{\sqrt{2}}C_s'\right]\Bigg], \end{aligned} \tag{A8}$$

where h_{V_i} and σ_{V_i} are the corresponding (dimensionless) coupling constants for a given ith octet. For simplicity we neglect any mixing between the octets.

[1] B. Aubert *et al.* (The *BABAR*), Phys. Rev. D **80**, 052002 (2009).
[2] P. del Amo Sanchez *et al.* (*BABAR* Collaboration), Phys. Rev. D **84**, 052001 (2011).
[3] A. E. Dorokhov, JETP Lett. **91**, 163 (2010).
[4] P. Kroll, Eur. Phys. J. C **71**, 1623 (2011).
[5] S. J. Brodsky, F.-G. Cao, and G. F. de Teramond, Phys. Rev. D **84**, 075012 (2011).
[6] S. J. Brodsky, F.-G. Cao, and G. F. de Teramond, Phys. Rev. D **84**, 033001 (2011).
[7] Y. N. Klopot, A. G. Oganesian, and O. V. Teryaev, Phys. Rev. D **84**, 051901 (2011).
[8] I. Balakireva, W. Lucha, and D. Melikhov, Phys. Rev. D **85**, 036006 (2012).
[9] A. Bakulev, S. Mikhailov, A. Pimikov, and N. Stefanis, Phys. Rev. D **84**, 034014 (2011).
[10] A. Dorokhov, arXiv:1109.3754; in Hadron Structure 11, Slovakia, Tatranská Štrba, July 1, 2011; in The Actual Problems of Microworld Physics (Gomel, Belarus, August 1 - 12, 2011); in International Workshop on $e+e-$ Collisions from Phi to Psi (Novosibirsk, Russia, September 19-22, 2011).
[11] P. Lichard, Phys. Rev. D **83**, 037503 (2011).
[12] H. R. Grigoryan and A. V. Radyushkin, Phys. Rev. D **77**, 115024 (2008).
[13] A. Stoffers and I. Zahed, Phys. Rev. C **84**, 025202 (2011).
[14] L. Cappiello, O. Cata, and G. D'Ambrosio, Phys. Rev. D **83**, 093006 (2011).
[15] S. Noguera and S. Scopetta, Phys. Rev. D **85**, 054004 (2012).
[16] Y. Bystritskiy, V. Bytev, E. Kuraev, and A. Ilyichev, Phys. Part. Nucl. Lett. **8**, 73 (2011).
[17] S. Noguera and V. Vento, Eur. Phys. J. A **46**, 197 (2010).
[18] G. Amelino-Camelia *et al.*, Eur. Phys. J. C **68**, 619 (2010).
[19] D. Babusci H. Czyż, F. Gonnella, S. Ivashyn, M. Mascolo, R. Messi, D. Moricciani, A. Nyffeler, G. Venanzoni, and KLOE-2 Collaboration, Eur. Phys. J. C **72**, 1917 (2012).
[20] J.-M. Bian *et al.*, Int. J. Mod. Phys. A **24**, 267 (2009).
[21] H. Czyż and S. Ivashyn, Comput. Phys. Commun. **182**, 1338 (2011).
[22] H. Czyż and E. Nowak-Kubat, Phys. Lett. B **634**, 493 (2006).
[23] K. Melnikov and A. Vainshtein, Phys. Rev. D **70**, 113006 (2004).
[24] J. Prades, E. de Rafael, and A. Vainshtein, in *Lepton Dipole Moments*, edited by Roberts, B. Lee, Marciano, and J. William, Advanced Series on Directions in High Energy Physics Vol. 20 (World Scientific, Singapore, 2009), p. 303.
[25] A. Nyffeler, Phys. Rev. D **79**, 073012 (2009).
[26] F. Jegerlehner and A. Nyffeler, Phys. Rep. **477**, 1 (2009).
[27] R. M. Carey *et al.*, Fermilab Proposal P-0989, 2009.
[28] T. Mibe (J-PARC $g-2$ collaboration), Chinese Phys. C **34**, 745 (2010).
[29] A. Bernstein and B. R. Holstein, arXiv:1112.4809.
[30] G. P. Lepage and S. J. Brodsky, Phys. Rev. D **22**, 2157 (1980).
[31] M. Knecht and A. Nyffeler, Eur. Phys. J. C **21**, 659 (2001).
[32] Z. K. Silagadze, Phys. Rev. D **74**, 054003 (2006).
[33] A. Khodjamirian, Eur. Phys. J. C **6**, 477 (1999).
[34] S. Agaev, V. Braun, N. Offen, and F. Porkert, Phys. Rev. D **83**, 054020 (2011).
[35] E. R. Arriola and W. Broniowski, Phys. Rev. D **81**, 094021 (2010).
[36] H. L. L. Roberts, C. D. Roberts, A. Bashir, L. X. Gutierrez-Guerrero, and P. C. Tandy, Phys. Rev. C **82**, 065202 (2010).
[37] E. Bartos, A. Dubnickova, S. Dubnicka, E. Kuraev, and E. Zemlyanaya, Nucl. Phys. **B632**, 330 (2002).
[38] A. E. Dorokhov, A. E. Radzhabov, and A. S. Zhevlakov, Eur. Phys. J. C **71**, 1702 (2011).
[39] V. Mateu and J. Portoles, Eur. Phys. J. C **52**, 325 (2007).
[40] K. Kampf and J. Novotny, Phys. Rev. D **84**, 014036 (2011).
[41] G. Ecker, J. Gasser, H. Leutwyler, A. Pich, and E. de Rafael, Phys. Lett. B **223**, 425 (1989).
[42] G. Ecker, J. Gasser, A. Pich, and E. de Rafael, Nucl. Phys. **B321**, 311 (1989).
[43] J. Prades, Z. Phys. C **63**, 491 (1994).
[44] K. Nakamura (Particle Data Group), J. Phys. G **37**, 075021 (2010).
[45] T. Feldmann, P. Kroll, and B. Stech, Phys. Rev. D **58**, 114006 (1998).
[46] T. Feldmann, Int. J. Mod. Phys. A **15**, 159 (2000).
[47] H. J. Behrend *et al.* (CELLO), Z. Phys. C **49**, 401 (1991).
[48] J. Gronberg *et al.* (CLEO), Phys. Rev. D **57**, 33 (1998).
[49] S. Ivashyn and A. Y. Korchin, Eur. Phys. J. C **54**, 89 (2008).
[50] S. Ivashyn and A. Korchin, Proc. Sci., EFT09 (2009) 055 [arXiv:0904.4823].
[51] S. Eidelman, S. Ivashyn, A. Korchin, G. Pancheri, and O. Shekhovtsova, Eur. Phys. J. C **69**, 103 (2010).
[52] M. Achasov *et al.*, Phys. Lett. B **559**, 171 (2003).
[53] S. J. Brodsky and G. P. Lepage, Phys. Rev. D **24**, 1808 (1981).
[54] L. Ametller, J. Bijnens, A. Bramon, and F. Cornet, Phys. Rev. D **45**, 986 (1992).
[55] F. Farzanpay *et al.*, Phys. Lett. B **278**, 413 (1992).
[56] R. Meijer Drees *et al.* (SINDRUM-I), Phys. Rev. D **45**, 1439 (1992).
[57] H. Berghauser *et al.*, Phys. Lett. B **701**, 562 (2011).
[58] R. Arnaldi *et al.* (NA60), Phys. Lett. B **677**, 260 (2009).
[59] G. Usai (NA60), Nucl. Phys. **A855**, 189 (2011).
[60] J. Wess and B. Zumino, Phys. Lett. B **37**, 95 (1971).
[61] E. Witten, Nucl. Phys. **B223**, 422 (1983).
[62] S. Actis *et al.*, Eur. Phys. J. C **66**, 585 (2010).